

Kinetic Modelling of Chromite Pellet Reduction with CO gas Under Rising Temperatures from 700 to 1520°C

Yanping XIAO, Markus REUTER

Delft University of Technology, Dept. of Applied Earth Science

Mijnbouwstraat 120, 2628 RX Delft, The Netherlands

Lauri HOLAPPA

Helsinki University of Technology, Laboratory of Metallurgy

Vuorimiehentie 2K, FIN-02015 HUT, Finland

ABSTRACT

Pre-reduction of chromite pellet is important for FeCr production in electric arc furnaces. As the charge descends, a single chromite pellet in the furnace is reduced with CO gas. To better understand the reduction mechanism, mathematical modelling of the reactions was carried out. In the present paper, the thermodynamic reducibility of the chromite constitutes with CO gas in the range of 700–1520°C was calculated. A structural grain model was modified and applied for simulating the reduction of a single chromite pellet with CO gas at rising temperatures. The calculated reduction rate agrees fairly well with the experimental measurements. The model describes satisfactorily the reduction process for reduction degree up to 30 percent. Based on the experimental information and the calculation results, the microstructure of the reduced pellets and the reaction mechanisms were illustrated and discussed. It could be concluded that for a single chromite pellet, the reduction is mixed controlled by pore diffusion and interfacial chemical reactions in the early stage, then after most of the iron oxides are reduced, the interfacial chemical reactions dominate the reduction process.

1 INTRODUCTION

The use of stainless steel is growing more rapidly than most of the other metals with an average annual increase of 4-5% during the last twenty years[1]. Ferrochrome, as the major constituent in stainless steels is one of the most rapidly growing primary metal products. Since the breakthrough of the AOD process, high carbon ferrochrome attained its position as the major chromium source for stainless steel. Submerged-arc furnaces are

used to smelt chromite ores into ferrochrome by the use of a suitable carbonaceous reductant (anthracite, char, coke). The process has been intensively developed during the years. Some recent developments to improve the efficiency of submerged-arc furnaces include closed top operation with utilisation of off-gas energy, computerised control to optimise power inputs, pelletised and pre-oxidised fines feed and optimising slag composition for maximum chromium recovery[2]. A schematic diagram of the furnace cross section is illustrated in Fig.1. Rather large temperature gradients exist in the furnace from a few hundreds at the surface of the burden to well over 2000 °C around the electrode tips, which creates various zones in the furnace forming a distribution of equilibria. In this industrial process, different reduction mechanisms exist in different reaction zones, due to large temperature gradients. Through analysing the slag from the ferrochromium smelting furnace, poor chromium recovery from partially reduced chromite spinels was observed. Knowing the reaction mechanism in each zone certainly can provide guidance for improving the reduction efficiency, getting better chromium yield and further decreasing the energy consumption.

Chromite reduction with CO gas is of practical significance in electric arc furnace for FeCr production process, which was experimentally proved to be possible when there is a carbon located nearby. In practice, a single chromite pellet experiences a rising temperature environment during the charge descending, which will be reduced by the upstream CO gas. The mathematical modelling of the reaction system is important for quantitatively interpreting the experimental data on laboratory scale, and further for providing a kinetic aid to improve the process with higher

chromium recovery. In addition, the modelling will certainly establish a fundamental basis for the FeCr process modelling and the furnace control, which affects the final output and the metallurgi-

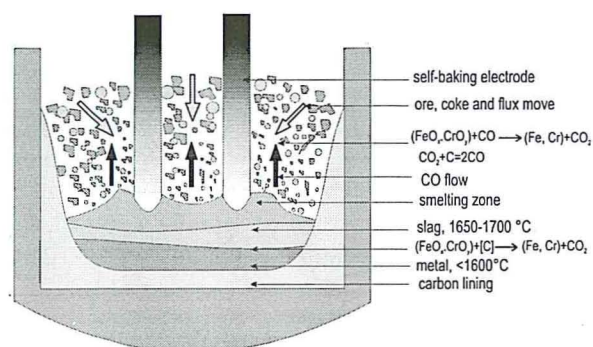


Fig.1 Schematic diagram of a cross section of a three electrodes electric arc furnace

cal memory of the furnaces. As a prerequisite to analyse the EAF furnace, and further to simulate the reduction progress within the furnace charge, it is essential to start from a single pellet.

There have been some attempts in the literature to discuss the reaction mechanism of the chromite reduction[3-5]. However, the mathematical modelling work on this reaction system is still in the preliminary stage. In author's previous work[6], the unreacted core model was applied for discussing the reaction mechanism of C-containing chromite pellet. This model was developed mainly for the dense particles and obviously could not be applied directly to describe the reduction of chromite pellet with CO gas. Based on the experimental information, a modified grain model was developed to mathematically simulate the chromite pellet reduction with CO gas at constant temperatures[7].

In the present paper, thermodynamic possibilities of chromite reduction with CO gas under rising temperature conditions will be evaluated. The modified reaction model for the behaviour of a single sintered chromite pellet under CO atmosphere will be presented. The modelling result will be compared to those from the experiments, and the reaction mechanisms will be discussed.

2 THERMODYNAMIC CONSIDERATION

Generally, chromite contains iron chromite (FeCr_2O_4), microchromite (MgCr_2O_4), magnetite (FeFe_2O_4), magnesium aluminate (MgAl_2O_4) and some silicate phases. In the sintering process iron in the pellet is mostly oxidised to trivalent state under air atmosphere. For the sintered pellet used in the present study, about 76% of the iron exist in trivalent state. Therefore the sintered chromite contains the following reducible constituents: Fe_2O_3 , Fe_3O_4 , $(\text{Fe}, \text{Cr})_2\text{O}_3$, FeCr_2O_4 and MgCr_2O_4 . Due to lack of thermodynamic data, the solid solution $(\text{Fe}, \text{Cr})_2\text{O}_3$ (about 7.8 mol%) possibly existed in the sintered chromite pellet is approximately considered as Fe_2O_3 and Cr_2O_3 . The reduction feasibility of the reducible constituents in the chromite has been thermodynamically analysed. The equilibrium partial pressure ratio of CO_2 to CO is represented in Fig.2 in the temperature range of 973 to 1923 K. The activities of the

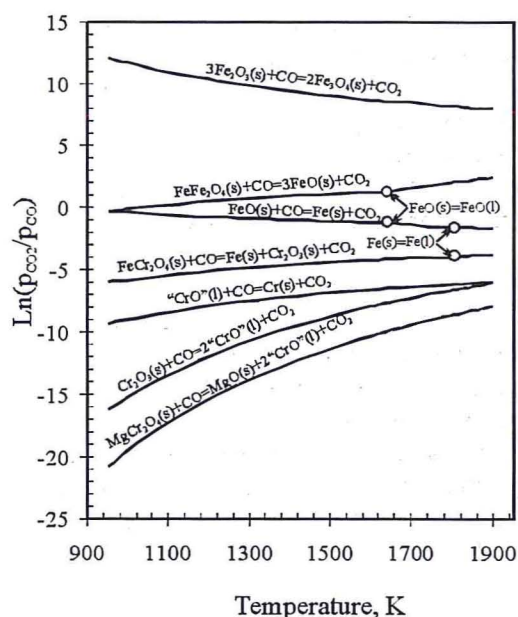


Fig.2 Equilibrium partial pressure ratio of CO_2 to CO for the reduction of the main constituents of chromite

solid reactants and products were assumed to be unity in the calculation. It can be seen that reduction of chromite pellet with CO is a very complicated process. It starts with reduction of iron oxides, and the chromium oxides will be reduced only at high temperatures and with low CO_2 to CO ratio.

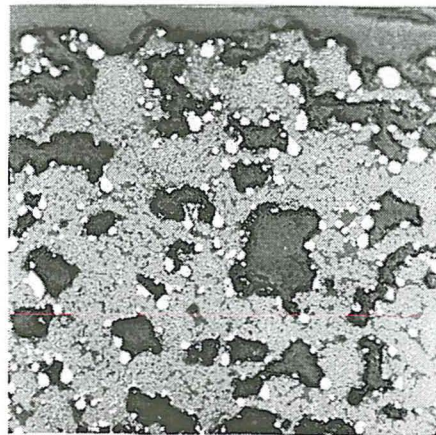
By comparing the equilibrium oxygen partial pressure, Fe_2O_3 in the pellet normally will be reduced first into magnetite, and magnetite $\text{Fe}_3\text{O}_4(\text{s})$ is easier to be reduced than iron chromite $\text{FeCr}_2\text{O}_4(\text{s})$. At the same temperature, the reduction tendency of $\text{FeCr}_2\text{O}_4(\text{s})$ is much higher than that of $\text{MgCr}_2\text{O}_4(\text{s})$, and the reduction of $\text{MgCr}_2\text{O}_4(\text{s})$ needs higher starting temperature than that of $\text{FeCr}_2\text{O}_4(\text{s})$. It should be pointed out that the "CrO"/Cr equilibrium presented in this figure is hypothetical, because divalent chromium oxide is not stable under the considered thermodynamic conditions. In the literature, multi-parallel reactions in a reaction model have not been found in the metallurgical field. The chromite particle in different location of the pellet usually may undergo different reactions. In the present work, this complex reaction characteristic is described by a global reaction, and the equilibrium constant is determined based on chromite composition, different equilibrium constants for the selective individual reactions of the reducible constituents in chromite, reaction temperature, and local reduction extent related to the thermodynamic reducibility.

3 EXPERIMENTS

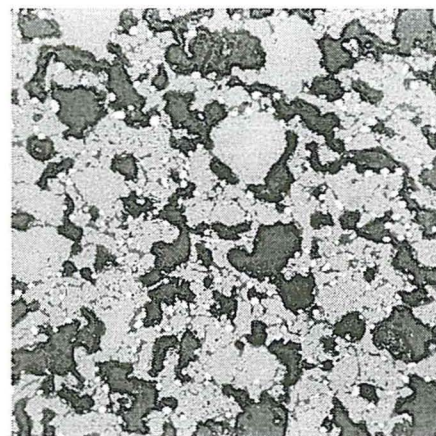
In the electric arc furnace, carbon free chromite pellet and lumpy ore are mainly pre-reduced with CO during the burden descending. The kinetic reactions of solid state reduction of chromite pellets with CO were experimentally studied by thermogravimetric analysis. The process pellets used in the experiments were made of Kemi chromite ore with an average analysis of 43% Cr_2O_3 , 19% Fe_{total} , 13.8% Al_2O_3 , 10.4% MgO , 4.2% SiO_2 and minor contents (<1%) CaO and oxides of Ti, Mn and Ni. The oxidation state of iron oxide varied in different samples, an average value 0.24 of $\text{Fe}^{2+}/\text{Fe}_{\text{total}}$ was chosen for the composition calculation. The pellet weight was about 3 g and the diameter was about 12 mm. The weight loss of the sample, which indicated the reduction rate, was continuously recorded during the experiment. The moisture-free pellet was first placed in the reaction zone at 700°C , then the temperature was program controlled with the rate of 2.5°C per minute from 700 to 1520°C , and

maintained at 1520°C for 2 hours. In the experiments, graphite cylinder with no contact to the sample was used to maintain a high reducing atmosphere around the sample. The reduction degree in the experiments was defined as percentage of the removed oxygen from the total removable oxygen in chromite. The experimental details were described earlier by Kekkonen et al.[8].

The microstructure of the reduced chromite pellet was examined with optical microscope through the pellet cross-section. It was observed that the sintered chromite pellet was partly reduced with CO at rising temperature condition, with different



(a) near the pellet surface



(b) in the pellet centre

Fig.3 Microstructure of the reduced chromite pellet at rising temperatures from 700 to 1520°C at a constant rate of $2.5^\circ\text{C}/\text{min}$, followed by 2 hours at 1520°C (white: metal, grey: chromite, black: silicate or pore)

reduction extent in outer and inner parts of the pellet. Fig.3a and Fig.3b show the microstructure of the pellet in the vicinity of the outer surface and inner part, respectively. As reduced product, bigger metal beads of the reaction product can be seen just beneath the surface, and they become smaller when going inside towards the pellet centre. Metal beads along the pellet cross section from different experiments were analysed with electron microprobe, and the distribution of iron and chromium in different zones at constant reaction temperatures (1420°C, 1520°C and 1595°C)

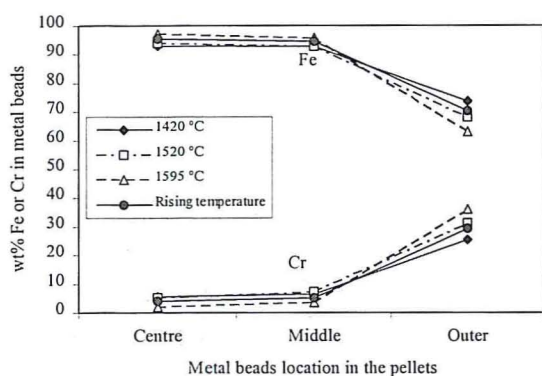


Fig.4 Iron and chromium contents in metal beads in different zones of the pellets reduced at different temperatures

and at rising temperatures (from 700 to 1520°C) is illustrated in Fig.4. The great difference in composition was found between the surface and the inner part of the pellet. In the outer zone metal has fairly high chromium content 25 – 36% whereas it is much lower in the half-radius region and still lower in the centre. The effect of temperature can be seen as well, the higher temperature the more chromium was reduced in the surface zone. It seems that CO diffuses through the pellet pore, and the reduction proceeds from the outer to the inner zone of the pellets. For the chromite particles (grain), the ore usually consists of relatively dense sub-grains that are separated by the pore network. Based on the study on the reduction of chromite lumpy ore, unreacted cores were partly observed from the SEM-photographs, especially at lower temperature. This provides the background for the reaction of the chromite grains in the pellet, i.e. the reduction proceeds in a relatively narrow zone, and the reaction interface

moves in a topochemical fashion from the external surface to the centre of the chromite grain.

Based on the above experimental observations, the structure grain model was modified to simulate the reaction of the chromite pellet with CO under rising temperature conditions.

4 REACTION MODEL

The reduction of chromite pellet with CO actually takes place between gases and porous solids which is characterised by different interrelated mechanisms or steps. Because certain physical parameters are not available and difficult to establish or estimate, the micro-level factors such as ionic diffusion and the rearrangement of the cations and anions were neglected. In general, a porous solid and gas reaction can proceed via the following steps:

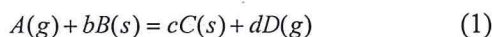
- 1 mass transfer of gaseous reactant through an external gas film surrounding the solid pellet;
- 2 diffusion of the gaseous reactant through the pellet pores, and further through the porous solid which consists of a mixture of solid reactants and products;
- 3 adsorption of the gaseous reactant on the surface of solid reactant;
- 3 chemical reaction at the surface of the solid reactant;
- 4 nucleation of the metal phase, diffusion and agglomeration on the local chromite grain surface;
- 6 desorption of the gaseous product from the surface of solid product;
- 7 diffusion of the gaseous product through the solid phase and through the pellet pores from the interior to the pellet surface;
- 8 mass transfer of gaseous product through the external gas film to bulk gas stream.

The significance of each step in the overall reaction depends on the reaction system and the specific experimental conditions.

In the present reaction model, it is assumed that a spherical pellet of the solid reactant consists of a large number of spherical chromite grains with uniform size which are surrounded by pores. The pellet sample is brought into contact with a reacting gas CO to form a solid product and a gaseous

product CO₂. The rate of adsorption and desorption of the reaction gas on the solid lattice is much faster than the chemical reaction rate. The reaction of each grain is assumed to follow the unreacted core model[6], i.e., the reaction front forms spherical symmetry within each grain and proceeds from the outer surface toward the centre inside. The reactant gas CO is first transferred from the bulk gas stream, it diffuses through the pores between the grains, and further diffuses through a solid product layer within each grain, and then reacts at the spherical reaction interface. When reduction results in metal formation metal atoms form nuclei in proper sites e.g. pore walls of the reaction zone. After nucleation, further reduction tends to occur on the existing nuclei where the diffusing ions of iron and chromium meet CO gas, and new metal is precipitated on the nuclei which thus grow to metal beads. It is assumed that this procedure proceeds fast enough not to be the controlling step of the reduction process. The generated product gas CO₂ diffuses outward through the solid product layer, and between the grains and finally transfer into the bulk gas stream. The overall rate of reaction is computed by summing up the contributions of all these individual grains.

If we express the gas reactant CO by *A*, the solid reactant chromite by *B*, the solid product by *C*, and the gas product by *D*, the reaction can be described as follows:



In this reaction model, it is assumed that the initial pellet size is maintained throughout the reaction. The structure of the porous matrix of the pellet normally will be altered by the chemical reaction and by sintering. The allowance is normally made up by considering the porosity and thus the tortuosity changes, i.e., the effect on the effective diffusivity. The unreacted core model describes the behaviour of a small particle, and the reaction between the gas and the solid is a reversible reaction of the first order. The schematic diagram of the structure of the grain model is shown in Fig.5, in which *R*₀ is the pellet radius, *R* is pellet radial coordinate, *r*_s is average grain size, and *r* is the grain reaction front. CO concentration is represented by *C*_A within the pellet, *C*_{A*R*0} at the pellet surface and *C*_{A0} in the bulk.

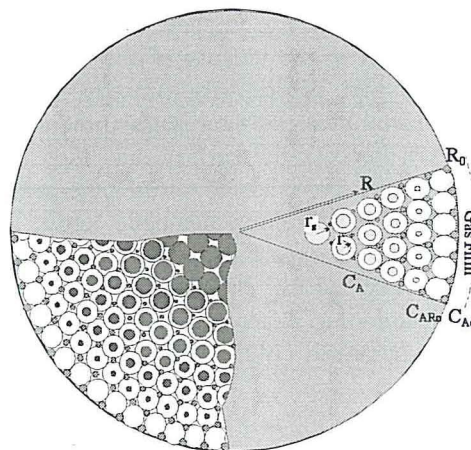


Fig.5 Schematic diagram of the grain model

At quasi-steady state, equimolar counter diffusion is assumed. The amount of gaseous reactant within the pores is negligible compared with the net input and the reaction consumption. ρ_m is molar density of the reducible oxygen in the initial chromite grain. P_0 is the pellet initial total porosity. The mathematical development of the model was described earlier by the authors[7]. The final governing equations of the model can be expressed as the following two differential equations:

$$\frac{dr}{dt} = -\frac{k}{\rho_m} \left(C_A \cdot \left(1 + \frac{D_A^c}{D_D^c \cdot K_E} \right) - \frac{1}{K_E} \left(C_{A_s} + \left(\frac{D_A^c}{D_D^c} - 1 \right) \cdot C_{A_{r_s}} \right) \right) \quad (2)$$

$$\frac{D_A^c}{R^2} \frac{\partial}{\partial R} \left(R^2 \frac{\partial C_A}{\partial R} \right) = 3(1 - P_0) \frac{r_s^2}{r^2} k \left(C_A \cdot \left(1 + \frac{D_A^c}{D_D^c \cdot K_E} \right) - \frac{1}{K_E} \left(C_{A_s} + \left(\frac{D_A^c}{D_D^c} - 1 \right) \cdot C_{A_{r_s}} \right) \right) \quad (3)$$

Here, *k*, the general reaction rate constant of the chromite grain, can be expressed as follows according to the unreacted core model,

$$\frac{1}{k} = \frac{1}{k_+} + \frac{r(r_s - r)}{r_s} \left(1 + \frac{D_{Ag}^c}{D_{Dg}^c K_E} \right) \frac{1}{D_{Ag}^c} \quad (4)$$

k₊ is the forward global reaction rate constant. *D*_{Ag}^{*c*} and *D*_{Dg}^{*c*} are the effective diffusivities of CO and CO₂ through the product layer of the chromite grain, respectively. *K*_E is the global equilibrium constant of the chemical reactions, and *t* represents reaction time.

The relationship between the reaction degree X , which correlated to the experimental measurement, and the local reduction extent for a chromite grain can be derived as follows:

$$X = \frac{3}{R_o^3} \int_0^{R_o} R^2 \left(1 - \frac{r^3}{r_s^3}\right) dR \quad (5)$$

In addition, to establish the initial and boundary conditions, it is assumed that no reaction has occurred before $t=0$, there is a symmetrical concentration profile at the centre of the pellet, and the molar flux at the outer surface of the pellet is continuous. Thus, the following initial and boundary conditions can be established:

$$\text{At } t=0, \quad r(R) = r_s \quad (6)$$

$$\text{At } R=0, \quad \frac{\partial C_A}{\partial R} = 0 \quad (7)$$

$$\text{At } R=R_o, \quad D_A^c \frac{\partial C_A}{\partial R} = h_m (C_{A_s} - C_A) \quad (8)$$

Here, h_m is the mass transfer coefficient of CO from the bulk gas stream to the surface of the chromite pellet.

The concentration profile, the reaction extent of the chromite grains at different radii of the pellet, and the reduction degree of the pellet can be calculated by solving the above equations using a finite difference technique.

5 MODEL PARAMETERS

Most of the model parameters were evaluated based on the experimental conditions or from the known correlation in the literature, only the global reaction rate constant k_+ , and its associated activation energy E_A were determined by fitting to the experimental results, as listed in Table 1.

According to the compositions of the sintered chromite pellet and the thermodynamic calculations on the reduction of the major constituents of chromite with CO, the fraction of the reducible oxygen in each reducible constitute to that in the chromite and the equilibrium constant were calculated and listed in Table 2. The global equilibrium constant was established based on thermodynamic reducibility (selective reduction steps), chromite

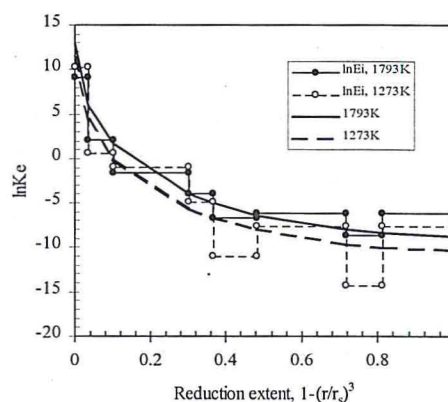


Figure 6 The relationship of the global equilibrium constant with local reduction extent of the chromite grain at 1793K and 1273K

compositions and the equilibrium constants of the chemical reactions of different reducible constituents in chromite with CO. Fig. 6 shows the relationship of the global equilibrium constant with reduction extent within chromite grain. The smooth line was mathematically correlated from the points defined by the chromite compositions (ρ_i/ρ_m) and the equilibrium constants of the indi-

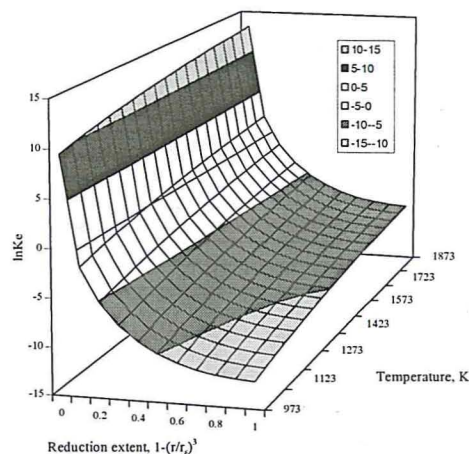


Figure 7 Global equilibrium constant with reduction extent and temperature

vidual chemical reactions in the chromite. Fig.7 demonstrates the three-dimension relationship among the global equilibrium constant, reduction extent within chromite grain and the reaction temperature, which was applied in the model calculation.

Considering diffusion effect in the pellet, the relationship among the total porosity, open porosity, tortuosity, temperature and reduction extent is important. During the reduction and sintering at high temperatures, the silicate phase could be softened and even melted, and the metal beads formed might to a certain extent fill the pores, hence the open porosity of the pellet might be changed. However it is very difficult to evaluate the structure parameters, especially the open porosity, based on the available experimental information. In the present calculation, the porosity was approximately assumed to be constant. Tortuosity was defined based on random pore model^[9]. The CO-CO₂ diffusivities were calcu-

lated by Chapman-Enskog equation^[10] and Dust Gas Model^[11]. Both the molecular and Knudsen diffusion have been taken into consideration in the model calculation.

The mass transfer coefficient of CO was calculated based on the data extrapolated from lower temperatures^[12]. In the experiments, the chromite pellets were observed to have no significant volume changes, therefore the pellet size and the grain size were assumed to be constant. The activation energy of the global reaction was determined to be 420 kJ/mole.

Table 1 Model parameters in the model calculation

Symbols	Value	Note
R	0.6 cm	Pellet radius, measured
r _s	30 μm	Grain size in average
P _g	0.10	Porosity in chromite grain
P ₀	0.28	Initial total porosity of the sintered pellet
P ₀ ^o	0.20	Initial open porosity of the sintered pellet
τ	1/P ^o	Tortuosity, based on random pore model ^[9]
ρ _m	0.0458 mole/cm ³	Molar density of the reducible oxygen in sintered chromite, calculated based on pellet compositions
C _{A0}	6.8×10 ⁻⁶ mole/cm ³	Bulk CO concentration at 1520°C
D _A	3.58×10 ⁻⁵ ·T ^{1.504} cm ² /s	CO and CO ₂ diffusivity, Calculated by Chapman-Enskog Equation ^[10] and Dust Gas Model ^[11] , combined effect of molecular and Knudsen diffusion
D _A ^c	D _A ·P ^o /τ cm ² /s	
D _D ^c	D _A ^c /1.25 cm ² /s	
h _m	6.368+0.00135T cm/s	Mass transf. coef. ^[12] from Sh=2.0+0.60(Re) ^{1/2} (Sc) ^{1/3}
Ln(K _E)	20.18×(1-(r/r _s) ³)-41.86×(1-(r/r _s) ³) ^{1/2} +16.97-7234/T	Global equilibrium constant, from K _E ⁱ , ρ _m ⁱ /ρ _m , based on reduction selectivity
k ₊	k ₊ =2.75×10 ¹² ·exp(-50520/T), cm/s	Arrhenius equation from experimental data fitting
E _A	420 kJ/mole	Activation energy of the global chemical reaction

Table 2 Major reactions of sintered chromite pellet with CO at 1520 °C

Reactions	ΔG ^o , J ^[13]	ρ _i /ρ _m	lnK _E ⁱ
3Fe ₂ O ₃ (s)+CO=2Fe ₃ O ₄ (l)+CO ₂ (g)	-42929-52.00T	0.0335	9.14
FeFe ₂ O ₄ (s)+CO=3FeO(l)+CO ₂ (g)	123979-85.98T	0.0671	2.03
Fe _{0.947} O(l)+CO=0.947Fe(s)+CO ₂ (g)	-48530+39.84T	0.2013	-1.54
FeCr ₂ O ₄ (s)+CO=Fe(s)+CO ₂ (g)+Cr ₂ O ₃ (s)	35739+12.62T	0.0616	-3.92
Cr ₂ O ₃ (s)+CO=2CrO(l)+CO ₂ (g)	160596-34.44T	0.1180	-6.64
CrO(l)+CO=Cr(s)+CO ₂ (g)	53211+21.40T	0.2361	-6.15
MgCr ₂ O ₄ (s)+CO=MgO(s)+2CrO(l)+CO ₂ (g)	203441-41.55T	0.0941	-8.66
CrO(l)+CO=Cr(s)+CO ₂ (g)	53211+21.40T	0.1883	-6.15

6 RESULTS AND DISCUSSION

The calculated reduction rate was compared to the measurements under the experimental conditions, and good agreement has been achieved, except for the final reduction stage. The result is shown in Fig.8. The concentration profile of CO gas and the reaction extent of the chromite grains along the radius of the pellet were calculated and are demonstrated in Figs. 9 and 10. According to these calculated results, it could be concluded that the chromite pellet reduction with CO gas is generally mixed controlled by various steps, including the pore diffusion, the global chemical reaction and the product layer diffusion within the chromite grain, as well as the gas phase mass transfer under the present experimental conditions. After most of

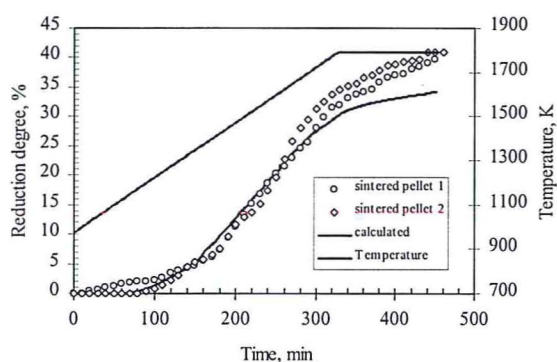


Figure 8 Comparison between measured and calculated reduction rate for process chromite pellet reduction with CO at rising temperatures

the iron oxides are reduced, the reduction is mainly controlled by interfacial chemical reactions. The activation energy for the reduction was determined to be 420 kJ/mole for sintered pellet under rising temperature condition.

In the modelling, a diffusion resistance was found to exist within the product layer of the chromite grain, but the effects are not so significant compared to the effects of pore diffusion and interfacial chemical reactions, especially in the earlier stage when the product layers are thin. Mass transfer of CO gas inward or CO₂ outward through the external gas film surrounding the pellet has very small effect on the reduction rate,

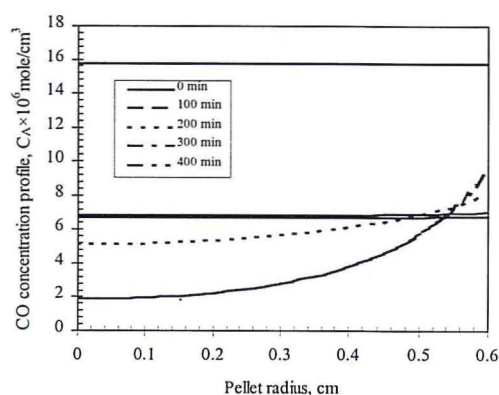


Fig.9 Calculated concentration profile of CO through the pellet for the reduction of green chromite pellet at 1520°C under experimental conditions

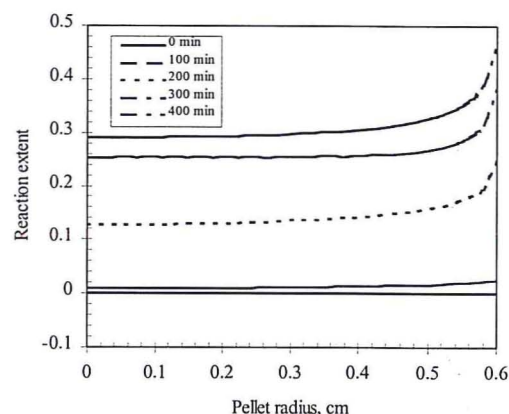


Fig.10 Calculated reaction extent of chromite grains for the reduction of green chromite pellet at 1520°C under experimental conditions

which was proved by changing CO gas flow rate in the experiments.

A concentration gradient of CO gas is formed in the pellet at lower temperatures, and the reaction takes place more rapidly near the pellet surface compared to the pellet interior. This agrees well with the experimental observations which showed that reduction occurred throughout the pellet, and the metallic beads found in the outer part of the pellet are bigger than that in the inner part.

The experimental results showed gradual composition changes of the Fe/Cr ratio from the analysis of the metal droplets across the pellet. This is understandable if activities of iron and chromium

oxides as well as the respective metal activities in the formed metal phase are taken into consideration. It is obvious that when iron oxide reduction has proceeded far enough, chromium oxide starts to be reduced and the metallic chromium formed dissolves in available Fe-based metal phase. According to the information on the reduction degrees of iron and chromium in the chromite in literature^[14], before the start of the chromium oxide reduction, about 40% of iron oxides have been reduced. Beyond that limit, the iron oxides and chromium oxide are reduced simultaneously. In general, this is in conformity with the philosophy of the global interfacial reaction.

The structure of pellets or even chromite grain is known to be a very important factor in solid state reduction. Pore diffusivity depends not only on the volume of pores but also their microstructure, open/closed porosity, pore diameter and tortuosity. Molecular or Knudsen diffusion can be dominant mechanisms depending on the structure. Morphology of the formed product layer, in this case iron-chromium metal alloy, can be an important factor as well. If metal is formed as a thin layer surrounding the unreacted core, the reduction rate can be greatly decelerated. This obviously is not the case. For the metal bead formation, atomic arrangement and new phase formation are important. To what extent this nucleation of the metal phase is rate controlling step still remains for discussion. Due to lowering reduction potential of the gas towards the centre of the pellet, problems in nucleation can be anticipated at least in the initial stage of the process at low temperatures. As a consequence, the unreacted core model for grains was only partly established.

When the porosity and the grain size vary in larger range, they may influence the reaction mechanism. Normally any increase in the porosity tends to speed up the reaction, except when the chemical reaction is the rate limiting step. Very small grains in principle would result in diffusion control, with the effective pore diffusivity being in the Knudsen region. Under the present investigation conditions, the porosity (open) in the outer part of the pellet may decrease more rapidly compared to the inner part of the pellet due to the higher reaction rate near the pellet surface. To obtain a quantitative relationship of the porosity changes during the reduction process, further experiments will be carried out. The chromite grains

in the experiment are not actually spherical in shape, and there exists a grain size distribution. The model could be improved by introducing a shape factor and a grain size distribution, and by considering the porosity changes in the pellet.

7 CONCLUSIONS

The reducibility of various constituents in the sintered chromite was thermodynamically analysed based on chromite composition and the reaction Gibbs free energy. Iron oxides will be reduced more easily than chromium oxides, and the chromium oxide in iron chromite will be reduced more easily than that in picchromite.

A modified structural grain model was developed which describes the chromite pellet reduction with CO gas under rising temperature conditions. A concept of a global chemical reaction was adopted which was contributed by the reactions of all the reducible constituents in the chromite. The activation energy was determined to be 420 kJ/mole. The calculated reduction rate was in a reasonable agreement with the experimental measurement.

For the reaction mechanisms, pore diffusion and interfacial reaction seem to dominate reduction kinetics at lower temperatures. At the later reduction stage at 1520 °C, the global chemical reaction could be the rate limiting step due to the low reducibility of chromium oxides in chromite.

ACKNOWLEDGEMENTS

The authors are grateful to Dr. M. Kekkonen and M.Sc. A-P. Syyrimaa from Helsinki University of Technology, Finland for providing the experimental information.

REFERENCES

1. Edwards, A. M., Developments in Technology for Ferrochromium Production. INFACON 8 Conference Proceedings, June 7-10, 1998, Beijing, China, pp.1-4.
2. Slatter, D.D., Technological Trends in Chromium Unit Production and Supply. INFACON

- 7 Conference Proceedings, June 11-14, 1995, Trondheim, Norway, pp.249-262.
3. Soykan, O., Eric, R.H. and King, R.P., Kinetics of the Reduction of Bushveld Complex Chromite Ore at 1416 °C. Metallurgical Transactions B, Volume 22B, December, 1991, pp.801 – 810.
 4. Van Vuuren, C.P.J., Bodenstein, J.J., Sciarone, M. and Kestens, P., The Reduction of Synthetic Iron Chromite in the Presence of Various Metal Oxides – A Thermo-analytical Study. INFACON 6 Conference Proceedings, 1992, Cape Town, S. Africa, pp.51-55.
 5. Niayesh, M.J. and Dippenaar, R.J., The Solid-state Reduction of Chromite. INFACON 6 Conference Proceedings, 1992, Cape Town, S. Africa, pp.57-63.
 6. Kekkonen, M., Xiao, Y. and Holappa, L., Kinetic Study on Solid State Reduction of Chromite Pellets. INFACON 7 Conference Proceedings, June 11-14, 1995, Trondheim, Norway, pp.351-360.
 7. Xiao, Y. and Holappa, L., Kinetic Modelling on Solid State Reduction of Chromite Pellet with CO. INFACON 8 Conference Proceedings, June 7-10, 1998, Beijing, China, pp.135-140.
 8. Kekkonen, M., Syynimaa, A., Holappa, L. and Niemela, P., Kinetic study on solid state reduction of chromite pellets and lumpy ores. The proceedings of INFACON 8 Conference, June, 1998, Beijing, China, pp.141-146.
 9. Bhatia, S.K. and Perlmutter, D.D., A Random Pore Model for Fluid-Solid Reactions: II. Diffusion and Transport Effects. AIChE J., Vol.27, No.2, 1981, pp.247-254.
 10. Hirschfelder, J.O., Curtiss, C.F. and Bird, R.B., Molecular Theory of Gases and Liquids. Wiley, New York, 1956.
 11. Mason, E.A., Malinauskas, A.P., and Evans, R.B., Flow and Molecules. Journal of Chemical Physics, Vol.46, No.8, 1967, pp.3199-3216.
 12. Incropera, F.P. and Dewitt, D.P., Fundamentals of Heat and Mass Transfer, 3rd edition, John Wiley & Sons, Singapore, 1990.
 13. Turkdogan, E.T., Physical Chemistry of High Temperature Technology, Academic press, London, 1980.
 14. McRae, S.S., An Investigation into Pelletizing and Prereduction of Transvaal Chromites. Proceedings of the 2nd International Symposium on Agglomeration, Atlanta, March 6-10, Vol.1, 1977, pp.356-377.